ELSEVIER

In vitro anti-*Trypanosoma cruzi* activity enhancement of curcumin by its monoketone tetramethoxy analog diveratralacetone

Julia M. Souza [a], Tatiana M. Vieira [b], Ana Carolina B.B. Candido [a], Daiane Y. Tezuka [c], G. Subba Rao [d], Sérgio de Albuquerque [c], Antônio E.M. Crotti [b], Jair L. Siqueira-Neto [e,**], Lizandra G. Magalhães [a,*]

[a] *Research Group on Natural Products, Center for Research in Sciences and Technology, University of Franca, Avenida Dr. Armando Salles de Oliveira, 201, Franca, CEP 14404-600, SP, Brazil*
[b] *Department of Chemistry, Faculty of Philosophy, Sciences and Letters at Ribeirão Preto, University of São Paulo, Av. Bandeirantes, 3900, Ribeirão Preto, CEP 14040-901, SP, Brazil*
[c] *School of Pharmaceutical Sciences of Ribeirão Preto, University of São Paulo, Av. do Café, s/n, Ribeirão Preto, CEP 14404-900, SP, Brazil*
[d] *Global Biotechnology Resource Center, 145 Rosewood Drive, Streamwood, IL, 60107, USA*
[e] *Skaggs School of Pharmacy and Pharmaceutical Sciences, University of California San Diego, San Diego, CA, 92093, USA*

ARTICLE INFO

ABSTRACT

Chagas disease is a tropical disease caused by the protozoan parasite *Trypanosoma cruzi* and currently affects millions of people worldwide. Curcumin (CUR), the major constituent of turmeric spice (dry powder of *Curcuma longa* L. plant rhizomes and roots), exhibits antiparasitic activity against protozoan parasites *in vitro*. However, because of its chemical instability, poor cellular uptake and limited bioavailability it is not suitable for clinical use. The objective of this study was to synthesize and evaluate *in vitro* CUR monoketone analog dibenzalacetone (DBA **1**) and its non-phenolic, methoxy (**2–4**) and chloro (**5**) derivatives for better stability and bioavailability against *T. cruzi*. Diveratralacetone, the tetramethoxy DBA (DBA **3**), was found to be the CUR analog with most enhanced activity against the amastigote forms of four strains of *T. cruzi* tested (Brazil, CA-I/72, Sylvio X10/4 and Sylvio X10/7) with 50% inhibitory concentration (IC$_{50}$) < 10 μM (1.51–9.63 μM) and selectivity index (SI) > 10 (C2C12 non-infected mammalian cells). This was supplemented by time-course assessment of its anti-*T. cruzi* activity. DBA **1** and its dimethoxy (DBA **2**) and hexamethoxy (DBA **4**) derivatives were substantially less active. The inactivity of dichloro-DBA (DBA **5**) was indicative of the important role played by oxygenated groups such as methoxy in the terminal aromatic rings in the DBA molecule, particularly at *para* position to form reactive oxygen species essential for anti-*T. cruzi* activity. Although the DBAs and CUR were toxic to infected mammalian cells *in vitro*, in a mouse model, both DBA **3** and CUR did not exhibit acute toxicity or mortality. These results justify further optimization and *in vivo* anti-*T. cruzi* activity evaluation of the inexpensive diveratralacetone for its potential use in treating Chagas disease, a neglected parasitic disease in economically challenged tropical countries.

1. Introduction

Trypanosomatids are unicellular organisms that colonize a wide diversity of environments and hosts (Stevens, 2008). Among the human diseases attributed to trypanosomatids is the American trypanosomiasis, commonly known as Chagas disease (CD) caused by *T. cruzi* (see Bern, 2015). The transmission of the disease occurs mainly by large blood-sucking reduviid bugs of the subfamily Triatominae. Other mechanisms of transmission include blood transfusion and vertical transfusion from mother to infant (Rassi et al., 2010). *Trypanosoma cruzi* infection can be divided into three phases. The first phase occurs shortly after transmission and can last up to two months. This acute phase can be asymptomatic or symptomatic but rarely fatal. The second phase is intermediate or indeterminate during which years may pass without the individual presenting clinical symptoms. The third phase is the chronic phase in which about 30% of the infected individuals will develop organ

malfunction without symptoms (20%) or develop cardiac and gastrointestinal manifestations (10%) (Guarner, 2019). Treatment of CD is still challenging since it is currently restricted to only two nitro drugs, benznidazole (BZ) and nifurtimox. While they are very efficient in treating acute infections, both drugs have frequent undesirable side effects and have limited efficacy in the chronic phase of the disease (Pérez-Molina & Molina, 2018).

Thus, the high impact on human health and its adverse effects of lost manpower and economic productivity worldwide emphasizes the urgent need for new drugs for the treatment of this neglected parasitic disease. In this context, it should be acknowledged that the phytotherapeutic use of natural products of plant origin in treating parasitic diseases has a long history in the indigenous herbal medical practice, particularly in the treatment of trypanosomiasis (Pereira et al., 2017). One such phytochemical agent identified is curcumin [(1*E*,6*E*)-1,7-bis(4-hydroxy-3-methoxyphenyl)-1,6-heptadiene-3,5-dione)] (CUR) (Fig. 1B), the major polyphenolic constituent of turmeric spice from *Curcuma longa* L. plant rhizomes and roots widely used in the global-favorite Indian curry powder with potent *in vitro* antiparasitic activity against trypanosomatid parasites (Cheraghipour et al., 2018). However, CUR is unstable in biological systems, poorly absorbed in the intestine and rapidly metabolized through reductive and conjugative processes which make it unsuitable for clinical use by the oral route (Cas & Ghidoni, 2019). Additionally, it can be either beneficial or harmful for the host depending on dose (Marathe et al., 2011). Although classified as a Pan-assay interference compound (PAIN) (Nelson et al., 2017), both *in vitro* and *in vivo* antiparasitic activities of CUR are well-established (Reddy et al., 2005; Magalhães et al., 2009; Gressler et al., 2015; Elamin et al., 2021). Thus, it might be interesting to explore the structure-activity relationship of new analogs based on the CUR chemical structure to identify better candidates for *T. cruzi* treatment.

The β-diketone (keto-enol) compounds are prone to rapid hydrolytic degradation which accounts for the instability of CUR in biological systems (Liang et al., 2009). To overcome this deficiency, recent studies with structural modifications have resulted in CUR analogs with its unstable β-diketone functionality replaced by monoketone moiety between the two terminal symmetric aromatic rings (Chakraborti et al., 2013; Shetty et al., 2015). These CUR monoketone analogs exhibit better stability and increased tissue uptake profile under both *in vitro* and *in vivo* experimental conditions (Liang et al., 2009). These modifications have

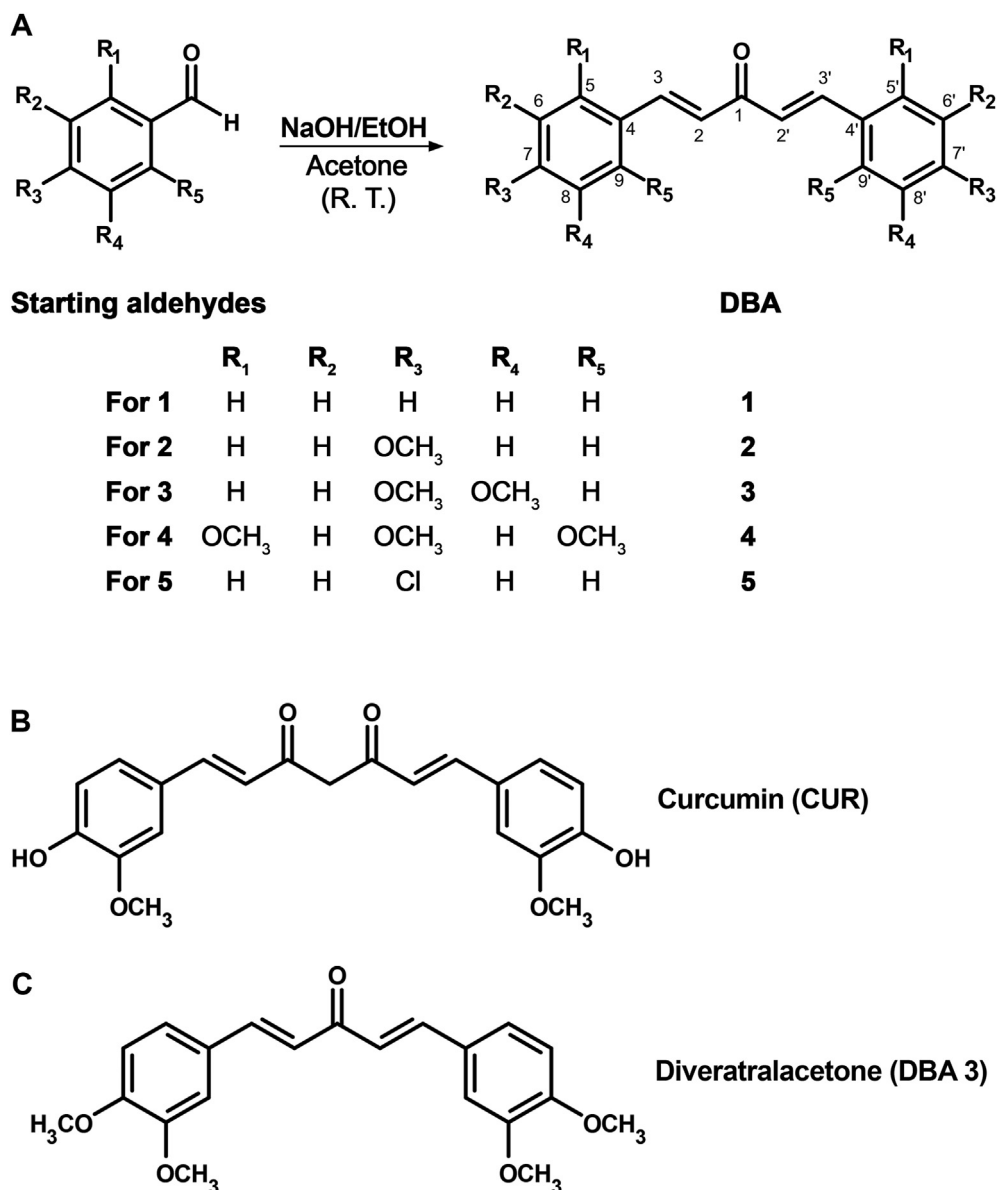|	R₁	R₂	R₃	R₄	R₅	
For 1	H	H	H	H	H	1
For 2	H	H	OCH₃	H	H	2
For 3	H	H	OCH₃	OCH₃	H	3
For 4	OCH₃	H	OCH₃	H	OCH₃	4
For 5	H	H	Cl	H	H	5

Fig. 1 A One-step synthesis of *trans*-dibenzalacetones (DBAs **1–5**). **B** Chemical structure of curcumin (CUR). **C** Chemical structure of diveratralacetone (DBA **3**).

resulted in their higher bioavailability with enhanced cytotoxic and anti-inflammatory activities (Liang et al., 2009; Arshad et al., 2017). Similar enhancement of antiparasitic activity *in vitro* has been observed with several monoketone analogs of CUR against protozoan parasites (Changtam et al., 2010; Alkhaldi et al., 2015; Chauhan et al., 2018; Carapina da Silva et al., 2019).

The present study reports the synthesis and anti-*T. cruzi* activity of dibenzalacetone (DBA **1**) and a series of its non-phenolic, methoxy (DBAs **2–4**) and chloro (DBA **5**) derivatives (Fig. 1A) against amastigotes and trypomastigotes of four strains of *T. cruzi* (Brazil, CA-I/72, Sylvio X10/4 and Sylvio X10/7) under *in vitro* experimental conditions. Benznidazole (BZ), a currently used drug to treat Chagas disease, and CUR were also tested alongside for reference and comparative purposes. Additionally, the cytotoxicity of the DBAs and CUR in two mammalian cell lines were evaluated *in vitro* and in a mouse model, and the most active DBA **3** and CUR were tested *in vivo* for acute oral toxicity. It is noteworthy that CUR-containing turmeric spice and CUR itself as yellow food color E100 are currently used worldwide, and both are considered safe for human consumption (Chainani-Wu, 2003; Chauhan et al., 2018). Further, the use of DBA **1** as an efficient UV blocker in sunscreens is approved by European Union and FDA in the USA (Thaman et al., 1996).

2. Materials and methods

2.1. Chemistry

2.1.1. General analytical methods

NMR spectra were recorded on a Bruker DRX-400 operating at 400 MHz for ^{1}H and 100 MHz for ^{13}C, respectively. CDCl$_3$ was used as solvent with reference solvent peaks at δ_H 7.26 and δ_C 77.10 ppm. Chemical shifts are in ppm (δ) and coupling constants (*J*) in Hz. Electrospray ionization mass spectrometry (ESI-MS) analyses were carried out on a Xevo TQS (Waters Assoc., Milford, MA, USA) tandem quadrupole mass spectrometer (QqQ) equipped with a Z-spray ionization source operating in the positive ion mode. High-resolution electrospray ionization mass spectra (HRESIMS) for compound **4** were obtained using a Bruker Daltonics MicrOTOF-Q IITM ESI-Qq-TOF (Billerica, MA, USA) in positive ion mode. Accurate masses were obtained using sodium trifluoroacetate (TFA⁻Na⁺) as the internal standard.

2.1.2. Synthesis of trans-dibenzalacetones

trans-Dibenzalacetone (DBA **1**) and its methoxy (DBAs **2–4**) and chloro (DBA **5**) derivatives were synthesized by Aldol condensation (Claisen-Schmidt reaction) of acetone and the appropriate methoxy/chloro aromatic aldehyde (Fig. 1A), as described in the literature (Vieira et al., 2018). The starting compounds benzaldehyde, 4-methoxybenzaldehyde (anisaldehyde), 3,4-dimethoxybenzaldehyde (veratraldehyde), 2,4,6-trimethoxybenzaldehyde and 4-chlorobenzaldehyde were purchased from Sigma-Aldrich, St. Louis, MO, USA. In general, a solution of sodium hydroxide (2.5 mol/l) and ethanol (20 ml) was added to a 100 ml-flask containing aromatic aldehyde (26 mM) and acetone (13 mM) at room temperature and stirred continuously for 1–24 h. The reaction mixture was then washed with cold water to remove excess base, and filtered under reduced pressure, dried under vacuum, and purified by recrystallization from hexane-ethanol mixture. The chemical structure of DBAs **1**–**5** was confirmed by NMR, EI-MS/HRESIMS and IR spectral analyses as described below.

Dibenzalacetone (DBA) (**1**): (1*E*,4*E*)-1,5-diphenylpenta-1,4-dien-3-one). C$_{17}$H$_{14}$O. Yield, 80%. Yellow powder, m.p. 109–111 °C (Lit: 113 °C) (Leow et al., 2014). ESI-MS (*m/z*, relative intensity): 235 [M + H]$^+$ (100%). NMR ^{1}H (400 MHz, CDCl$_3$): δ 7.10 (2H, *d*, $J_{2;3=2';3'}$ = 16.0, H2 = H2'), 7.76 (2H, *d*, $J_{3;2=3';2'}$ = 16.0, H3 = H3'), 7.62 (2H, *m*, H5 = H5' = H9 = H9'), 7.42 (2H, *m*, H6 = H6' = H8 = H8'), 7.40 (2H, *m*, H7 = H7'). ^{13}C (100 MHz, CDCl$_3$): δ 125.6 (CH, C2), 128.5 (CH, C5 = C5' = C9 = C9'), 129.1 (CH, C6 = C6' = C8 = C8'), 130.6 (CH, C7 = C7'), 132.8 (CH, C7), 134.9 (C, C4), 143.4 (CH, C3 = C3'), 189.0 (C = O, C1).

Dimethoxy-DBA (dianisalacetone) (**2**): [(1*E*,4*E*)-1,5-bis(4-methoxyphenyl)penta-1,4-dien-3-one]. C$_{19}$H$_{18}$O$_3$. Yield, 64%. Yellow powder, m.p. 143–145 °C (Lit: 128–130 °C) (Weber et al., 2005). ESI-MS (*m/z*, relative intensity): 295 [M + H]$^+$ (100%). NMR ^{1}H (400 MHz, CDCl$_3$): δ 3.85 (3 H, *s*, H10 = H10'), 6.93 (4 H, *d*, $J_{6,5=6',5'}$ = 8.7, H6 = H6' = H8 = H8'), 6.96 (2 H, *d*, $J_{2,3=2',3'}$ = 15.8, H2 = H2'), 7.56 (4H, *d*, $J_{5,6=5',6'}$ = 8.7, H5 = H5' = H9 = H9'), 7.71 (2 H, *d*, $J_{3,2=3',2'}$ = 15.8, H3 = H3'). ^{13}C (100 MHz, CDCl$_3$): δ 55.4 (CH$_3$, C10 = C10'), 114.6 (CH, C6 = C6' = C8 = C8'), 123.2 (CH, C3 = C3'), 127.5 (C, C4 = C4'), 129.7 (CH, C5 = C5' = C9 = C9'), 142.4 (CH, C3 = C3'), 161.4 (C, C7 = C7'), 188.6 (C = O, C1).

Tetramethoxy-DBA (diveratralacetone) (**3**): [(1*E*,4*E*)-1,5-bis(3,4-dimethoxyphenyl)penta-1,4-dien-3-one]. C$_{21}$H$_{22}$O$_5$. Yield, 83%. Yellow powder, m.p. 125–127 °C (Lit: 93–95 °C) (Leow et al., 2014). ESI-MS (*m/z*, relative intensity): 355 [M + H]$^+$ (100%). NMR ^{1}H (400 MHz, CDCl$_3$): δ 4.00 (12 H, *s*, H10 = H10' = H11 = H11'), 6.80 (2 H, *d*, $J_{6,5=6',5'}$ = 8.3, H6 = H6'), 6.98 (2 H, *d*, $J_{2,3=2',3'}$ = 15.8, H2 = H2'), 7.16 (2H, *d*, $J_{9,5=9',5'}$ = 1.8, H9 = H9'), 7.22 (2 H, *dd*, $J_{5,6=5',6'}$ = 8.3 e $J_{5,9=5',9'}$ = 1.8, H5 = H5'), 7.70 (2H, *d*, $J_{3,2=3',2'}$ = 15.8, H3 = H3'). ^{13}C (100 MHz, CDCl$_3$): δ 55.9 (CH$_3$, C10 = C10' = C11 = C11'), 110.0 (CH, C9 = 9'), 111.0 (CH, C6 = C6'), 123.0 (CH, C5 = C5'), 123.5 (CH, C2 = C2'), 127.8 (C, C4 = C4'), 142.9 (CH, C3 = C3'), 149.2 (C, C8 = C8'), 151.6 (C, C7 = C7') 188.4 (C = O, C1).

Hexamethoxy-DBA (**4**): [(1*E*,4*E*)-1,5-bis-(2,4,6-trimethoxyphenyl) penta-1,4-dien-3-one]. C$_{23}$H$_{26}$O$_7$. Yield, 97%. Yellow powder, m.p. 121–124 °C. ESI-MS (*m/z*, relative intensity): 415 [M + H]$^+$ (100%). HRESIMS: calcd. for C$_{23}$H$_{27}$O$_7$ [M + H]$^+$: 415.1751 found 415.1762. NMR ^{1}H (400 MHz, CDCl$_3$): δ 3.88 (18 H, *d*, H10 = H10' = H11 = H11' = H12 = H12'), 6.12 (4 H, *s*, H6,8 = H6,8'), 7.07 (2 H, *d*, $J_{2,3;2';3'}$ = 16.5, H2 = H2'), 7.94 (2H, *d*, $J_{3,2;3';2'}$ = 16.5, H3 = H3'). ^{13}C (100 MHz, CDCl$_3$): δ 56.2 (CH$_3$, C10 = C10' = C11 = C11' = C12 = C12'), 90.2 (CH, C6 = C6' = C8 = C8'), 106.1 (CH, C2 = C2'), 128.0 (C, C4 = C4'), 135.4 (CH, C3 = C3'), 161.9 (C, C7 = C7'), 163.5 (C5 = C5' = C9 = C9'), 201.1 (C = O, C1).

Dichloro-DBA (**5**): [(1*E*,4*E*)-1,5-bis(4-chlorophenyl)penta-1,4-dien-3-one]. C$_{17}$H$_{12}$Cl$_2$O. Yield, 44%. Yellow powder, m.p. 195–197 °C (Lit: 193 °C) (Vanchinathan et al., 2011). ESI-MS (*m/z*, relative intensity): 303 [M + H]$^+$ (100%). NMR ^{1}H (400 MHz, CDCl$_3$): δ 7.05 (2 H, *d*, $J_{2,3;2';3'}$ = 16.0, H2 = H2'), 7.40 (4H, *d*, $J_{5,6=5',6'}$ = 8.5, H5 = H5' = H9 = H9'), 7.55 (4 H, *d*, $J_{6,5=6',5'}$ = 8.5, H6 = H6' = H8 = H8'), 7.68 (2 H, *d*, $J_{3,2=3',2'}$ = 16.0, H3 = H3'). ^{13}C (100 MHz, CDCl$_3$): δ 126.0 (CH, C2 = C2'), 129.4 (CH, C6 = C6' = C8 = C8'), 129.7 (CH, C5 = C5 = C9 = C9'), 133.3 (C, C4 = C4'), 136.6 (C, C7 = C7'), 142.2 (CH, C3 = C3'), 188.6 (C = O, C1).

2.2. Parasites, mammalian cells and cell cultures

Four strains of *T. cruzi* parasites were selected for evaluation in this study. The Brazil strain tested consistently produces 100% mortality in mice between 9 and 14 days after the subcutaneous inoculation of 10^5 trypomastigotes/ml (Raether & Seidenath, 1983). The CA-I/72 strain used is the clone 72 derived from the CA-I strain, originally isolated from a man with chronic myocarditis in the Province of San Luis, Argentina in 1974. It has partial resistance to treatment with trypanocidal drugs BZ and nifurtimox (Nozaki et al., 1996). The Sylvio X10/4 and Sylvio X10/7 strains used are clones of the Sylvio X10 strain from Pará, Brazil. The Sylvio X10/4 strain, after reaching the acute stage, induces a chronic non-fatal phase in experimental mice, while the Sylvio X10/7 strain is responsible for inducing a fatal acute phase in mice (Postan et al., 1983).

Trypanosoma cruzi (Brazil, CA-I/72, Sylvio X10/4 and Sylvio X10/7 strains) parasites were cultivated as amastigote forms with C2C12 (murine muscle myoblast) cells at 37 °C in an atmosphere of 5% CO$_2$ in Dulbecco's Minimal Essential Medium (DMEM) (Gibco, Grand Island, NY, USA) supplemented with 10% heat-inactivated fetal bovine serum (FBS) (Sigma-Aldrich), 25 mM [4-(2-hydroxyethyl)-1-piperazineethanesulfonic acid] (HEPES), penicillin and streptomycin (Gibco), at pH 7.2, and sub-cultured every 7 days. *Trypanosoma cruzi* (Sylvio X10/4 strain) trypomastigote forms were obtained from supernatant of amastigotes culture.

The LLC-MK$_2$ (monkey kidney fibroblasts) cells were cultivated in Roswell Park Memorial Institute (RPMI) medium (Gibco) supplemented with 10% FBS at 37 °C with 5% CO$_2$. For cytotoxicity studies, the following mammalian cells were used: C2C12 and LLC-MK$_2$ with or without infection with *T. cruzi* parasites.

2.3. Anti-*T. cruzi* activity

2.3.1. Trypanocidal activity against trypomastigotes of T. cruzi

An initial screening against trypomastigotes of *T. cruzi* (Sylvio X10/4 strain) was performed as described previously with some modifications (de Menezes et al., 2016). Briefly, trypomastigotes of the parasite were seeded at 1×10^6 cells per well in 384-well plates. DBAs **1**–**5** and CUR in dimethyl sulfoxide (DMSO) (Sigma-Aldrich) solvent (0.19–100 μM) (0.1% DMSO) were added to the wells using Acoustic Transfer System (ATS) (Biosero, San Diego, CA, USA). The plates were incubated at 37 °C under 5% CO$_2$ for 72 h. Then, parasite viability was determined using resazurin blue dye (Sigma-Aldrich) (40 μM in PBS) by measuring the fluorescence intensity at 530 nm and 630 nm using EnVision 2105 Multimode Plate Reader (Perkin-Elmer). As positive and negative controls, parasites were incubated with BZ at concentrations 0.019–10 μM (2-fold dilution) and DMSO (0.1%), respectively.

2.3.2. Trypanocidal activity against amastigotes of T. cruzi

The parasite viability screening of DBAs **1**–**5** and CUR (Sigma-Aldrich) was performed using *T. cruzi* Sylvio X10/4 strain which was followed by testing with *T. cruzi* Brazil, CA-I/72, and Sylvio X10/7 strains. The screening assays were performed using a previously reported protocol with slight modifications (Ekins et al., 2015). Trypomastigotes were seeded with C2C12 cells with 1:15 infection rate in 384-well plates (Greiner Bio-One GmbH, Frickenhausen, Germany), using a FlexDrop™ liquid handler (Perkin-Elmer, San Jose, CA, USA). DBAs **1**–**5** and parent CUR in DMSO (Sigma-Aldrich) (0.19–100 μM, 2-fold dilution, 0.1% DMSO) were added to the wells using ATS. The plates were incubated at 37 °C under 5% CO$_2$ (trypomastigotes) for 72 h. The cells and parasites were then stained with 0.2 mg/ml of 4′,6-diamidino-2′-phenylindole dihydrochloride (DAPI) (Sigma-Aldrich) fluorescent stain solution for 2 h. Automated confocal microscope, ImageXpress® Micro Confocal High-Content Imaging System (MolDev, Sunnyvale, CA, USA) was used to take images; these were analyzed using the software *MetaXpress* version 5.3.0.5 for Windows (MolDev). The host cells and intracellular amastigotes were differentiated by the size of their DAPI-stained nuclei (125 μm^2 and 1–2 μm^2, respectively). Then, the growth inhibition was assessed by comparison to untreated controls (Ekins et al., 2015). As positive and negative controls, parasites and cells were incubated with BZ (Sigma-Aldrich) at concentrations 0.019–10 μM (2-fold dilution) and DMSO solvent (0.1%), respectively.

2.3.3. Time-course study against amastigotes of T. cruzi

The time course of anti-*T. cruzi* activity was performed as described above (Section 2.3.2) with intracellular amastigotes form of *T. cruzi* CA-I/72 strain which is known to exhibit partial resistance to BZ (Nozaki et al., 1996). DBAs **1**–**5** and CUR in DMSO solvent (0.19–100 μM, 2-fold dilution, 0.1% DMSO) were added to the plate after 48 h of incubation. The plates were then incubated at 37 °C under 5% CO$_2$ for 8, 12, 24 and 48 h, and growth inhibition determined by DAPI staining as described above. As positive and negative controls, parasites plus cells were incubated with BZ at concentrations 0.019–10 μM (2-fold dilution) and DMSO (0.1%), respectively.

2.4. Cytotoxic activity in infected and non-infected mammalian cells

The cytotoxicity in infected C2C12 mammalian cells was assessed by the same procedure used for anti-*T. cruzi* assays (Sections 2.3.2 and 2.3.3). Host cell viability was assessed based on the total number of cells divided by the average number of cells from negative controls (0.1% DMSO).

The cytotoxicity in non-infected C2C12 and LLC-MK$_2$ mammalian cells was assessed using the *in vitro* toxicology colorimetric assay Kit (MTT, Invitrogen ™, Thermo Fisher Scientific, Eugene, OR, USA). For these experiments, 5×10^4 cells were plated onto 96-well plates. After 24 h, DBAs **1**–**5** and CUR in DMSO solvent were added to each well at concentrations ranging from 0.19 to 100 μM (2-fold dilution, 0.1% DMSO). Negative (without treatment), solvent (DMSO 0.4%), and positive (Triton 15%) (Bio Agency, São Paulo, Brazil) controls were used. After incubation at 37 °C for 72 h, the medium was removed, the cells were washed with PBS, and 3-(4,5-dimethylthiazol-2-yl)-2,5-diphenyltetrazolium bromide (MTT) (2 mg/ml) was added to each well. The microplates were then covered and incubated at 37 °C for 4 h. Then, the cell viability was assessed by measuring NAD(P)H-dependent oxidoreductase enzyme activity. This was accomplished by determining the absorbance of the sample by a multi-plate reader (Microplate Reader Synergy H1, Biotek, Vermont, USA) at a test wavelength of 450 nm and a reference wavelength of 620 nm.

2.5. In vivo toxicity study in mice

2.5.1. Animals

Female BALB/c mice weighing between 25 and 30 g were maintained under controlled conditions of temperature (20–22 °C), humidity (10–50%), and 12 h light/dark cycle with *ad libitum* access to water and standard rodent chow (Labina, São Paulo, Brazil).

2.5.2. Acute toxicity test

The study was performed according to Organization for Economic Cooperation and Development (OECD) test guideline 423 (OECD, 2002) with slight modifications. Five groups of five 6-week-old female mice were used: Group I [diluent Tween 80/ethanol/water (7:3:90)]; Group II (DBA **3**, 300 mg/kg dose); Group III (DBA **3,** 1,000 mg/kg dose); Group IV (CUR, 300 mg/kg dose); and Group V (CUR, 1, 000 mg/kg dose). DBA **3** was chosen for this experiment because it showed the highest activity against all parasites tested and CUR was used as a reference compound.

DBA **3**, CUR and the solvent vehicle were administered orally (*p.o.*) as a single dose of 300 mg/kg or 1,000 mg/kg. Although the OECD guideline suggests the oral doses of 300 and 2,000 mg/kg, our dose selection was based on an earlier study which found CUR to be non-toxic in mice and rats at doses up to 5,000 mg/kg *p.o.* during a 14-days acute toxicity test (Aggarwal et al., 2016).

Clinical signs of toxicity (e.g. general appearance, ataxia, vocal fremitus, irritability, body tone, tremor, salivation, tearing, palpable ptosis, seizures and abnormal movements) were monitored continuously for 1 h after the administration, periodically during the first 24 h and then, daily for a total of 14 days (Da Silva et al., 2016; Saldanha et al., 2018).

2.6. Statistical analyses

The 50% inhibitory concentration (IC$_{50}$) was obtained by the infection ratio normalized by positive and negative controls. The 50% cytotoxic concentration (CC$_{50}$) was obtained by counting C2C12 cells infected with intracellular amastigotes of *T. cruzi* (Sections 2.3.2 and 2.3.3) or by viability of non-infected C2C12 and LLC-MK$_2$ cells (Section 2.4). Both IC$_{50}$ and CC$_{50}$ values were calculated with the aid of sigmoid dose–response curves, and the selectivity index (SI) values were determined by CC$_{50}$/IC$_{50}$ (Londero et al., 2018). Time course of anti-*T. cruzi* activity was analyzed by linear regression and one-way analysis (ANOVA), with multiple comparisons using the test for linear trend between column mean and left-to-right column order. All analyses were performed using Graphical Prism (version 8.0) (GraphPad Software, San Diego, CA, USA). Data represent the mean number ± standard deviation (SD) of three independent experiments performed in triplicate or as indicated.

3. Results

3.1. Synthesis of trans-dibenzalacetones

Synthesis of *trans*-dibenzalacetones (DBAs **1**–**5**) involved simple, one-step Aldol condensation reactions at room temperature using readily available, inexpensive starting chemicals, such as benzaldehyde, anisaldehyde and veratraldehyde (Fig. 1A) with high yields (up to 97%). They were easily purified by recrystallization using common solvents. All are stable compounds and safely storable at room temperature (Chauhan et al., 2018; Carapina da Silva et al., 2019).

3.2. Activity against trypomastigotes and amastigotes of T. cruzi

Initially, the trypanocidal activity of DBA **1**, its methoxy (DBAs **2**–**4**) and chloro (DBA **5**) derivatives were evaluated against trypomastigotes Sylvio X10/4 strain after 72 h. As shown in Table 1, DBA **3** showed the highest activity against the trypomastigotes ($IC_{50} = 11.54 \mu M$). DBAs **1**, **2** and **5** exhibited lower activities against trypomastigotes (IC_{50} range: 29.82–73.68 μM) while DBA **4** was inactive ($IC_{50} > 100 \mu M$). Reference compound CUR also demonstrated potent anti-*T. cruzi* activity against trypomastigotes ($IC_{50} = 9.89 \mu M$) and BZ exhibited high activity ($IC_{50} = 1.16 \mu M$).

Next, DBAs **1**–**5** were evaluated against amastigotes of *T. cruzi* Sylvio X10/4, followed by testing with amastigotes of *T. cruzi* Brazil, CA-I/72, and Sylvio X10/7 strains after 72 h incubation (Table 1). DBA **3** also exhibited the highest activity against the amastigote forms in all *T. cruzi* strains (IC_{50} range: 1.51–9.63 μM), except to Sylvio X10/7 strain. DBA **2** exhibited the highest activity against Sylvio X10/7 strain ($IC_{50} = 0.48 \mu M$) followed by DBAs **3** and **1** (IC_{50} range: 4.87 and 11.72 μM, respectively). DBA **4** exhibited an IC_{50} of 5.01 μM against CA-I/72, 33.07 μM against Sylvio X10/7 and no activity against Sylvio X10/4 and Brazil strains ($IC_{50} > 100 \mu M$). On the other hand, DBA **5** exhibited an IC_{50} higher than 20 μM against the amastigote forms in all *T. cruzi* strains (IC_{50} range: 25.29.51–73.68 μM), except for the Brazil strain ($IC_{50} = 6.37 \mu M$).

Concurrently run trypanocidal activities of the reference CUR and the positive control BZ against the four strains of *T. cruzi* amastigotes showed ranges for IC_{50} of 2.71–20.04 μM and 1.19–4.12 μM, respectively. Both compounds showed potent anti-*T. cruzi* activity against the CA-I/72 strain (IC_{50} of 2.71 and 2.02 μM, respectively) comparable to DBA **3** ($IC_{50} = 1.51 \mu M$) (Table 1).

3.3. Time course of trypanocidal activity against T. cruzi intracellular amastigotes of CA-I/72 strain and of cytotoxicity in C2C12-infected mammalian cells

The time-dependent (8–48 h) IC_{50} values of DBAs **1**–**5** against *T. cruzi* intracellular amastigotes (CA-I/72 strain) are given in Table 2. All DBAs **1**–**5** and the reference compound CUR were devoid of trypanocidal activity at the 8 h incubation period except for BZ ($IC_{50} > 10 \mu M$). DBA **1**

and DBA **3** showed anti-*T. cruzi* activity after 12 h of incubation (IC_{50} values of 76.78 and 63.30 μM, respectively). DBA **3** was the most active at 48 h of incubation with an IC_{50} value of 3.72 μM followed by DBAs **1** and **4** (IC_{50} values of 14.61 μM and 34.47 μM, respectively). In contrast, DBAs **2** and **5** lacked trypanocidal activity in any of the incubation times evaluated (8–48 h), all with $IC_{50} > 100 \mu M$. The reference CUR exhibited trypanocidal activity after 48 h of incubation ($IC_{50} = 2.25 \mu M$). In contrast, the positive control BZ showed gradual increase in trypanocidal activity with time (incubation period of 8–24 h) with $IC_{50} > 1.54$–10 μM.

As shown in Table 2, all DBAs tested (except DBA **4**), the reference compound CUR, and the positive control BZ showed cytotoxic activity in C2C12 cells infected with intracellular amastigotes of *T. cruzi* (CA-I/72 strain) after incubation of 8 h, with CC_{50} values ranging between 93.29 and 12.20 μM. After 48 h of incubation, all DBAs, CUR and BZ showed CC_{50} values of <1 μM. Another parameter evaluated was the selectivity index (SI), and the SI values obtained in the time-course evaluation were <1 for all DBAs, the reference compound CUR, and the positive control BZ.

Fig. 2 shows that DBAs **1**, **3**, and **4**, the reference compound CUR and the positive control BZ showed significant ($P < 0.05$ to $P < 0.0001$) time-dependent trypanocidal activity against intracellular amastigotes of *T. cruzi* (CA-I/72 strain). On the other hand, all compounds tested showed significant ($P < 0.05$ to $P < 0.0001$) time-dependent cytotoxic activity in C2C12 cells infected with intracellular amastigotes (CA-I/72) (Fig. 2).

3.4. Cytotoxicity in infected and non-infected mammalian cells

Table 3 lists the cytotoxicity of DBAs **1**–**5** in C2C12 cells infected with intracellular amastigotes of *T. cruzi* Brazil, CA-I/72, Sylvio X10/4 and Sylvio X10/7 strains. The DBAs **1**–**5** showed CC_{50} values between 15.46 and 0.09 μM in cells infected with all four strains of the parasite. The reference compound CUR and the positive control BZ tested in the same assay exhibited CC_{50} of 6.71–1.91 and > 10 μM, respectively. The DBAs presented SI values between 0.01 and 2.25 for all four strains evaluated; these results were comparable with the values obtained for the reference compound CUR (0.09–2.47).

Additionally, the cytotoxic activity of DBAs **1**–**5** in two non-infected cell lines, C2C12 and LLC-MK$_2$, were evaluated (Table 4). In general, among the five DBAs evaluated, those with the strongest activity against *T. cruzi* parasites were also found to be the most cytotoxic. Thus, DBA **3** showed CC_{50} values of 20.82 and 11.51 μM in C2C12 and LLC-MK2, respectively, followed by DBAs **1**, **2**, **4** and **5** (all were less toxic than DBA **3**). The reference CUR exhibited CC_{50} of 18.03 and 32.49 μM, in C2C12 and LLC-MK2, respectively. The positive control BZ was the least toxic in the two non-infected cell lines tested (CC_{50} of 37.85 and 167.50 μM, respectively). In non-infected C2C12 cells, DBAs **3** and **4** showed the highest SI values of 13.78 and 10.71, respectively among all DBAs tested (Table 4). Similarly, in non-infected LLC-MK$_2$ cells, DBAs **3** and **4** among the DBAs along with CUR exhibited the highest SI values of 7.62, 10.00 and 11.98, respectively (Table 4). The positive control BZ

Table 1

In vitro anti-*T. cruzi* activity (IC_{50}) of DBAs against trypomastigotes of Sylvio X10/4 strain and amastigotes of Brazil, CA-I/72, Sylvio X10/4 and Sylvio X10/7 strains after 72 h incubation

DBA	IC_{50} (μM) ± SD				
	Trypomastigotes	Amastigotes			
	Sylvio X10/4 strain	Brazil strain	CA-I/72 strain	Sylvio X10/4 strain	Sylvio X10/7 strain
1	41.24 ± 2.25	21.05 ± 2.51	4.67 ± 1.96	33.98 ± 2.92	11.72 ± 0.81
2	29.82 ± 2.12	51.59 ± 4.90	17.46 ± 1.06	46.58 ± 0.48	0.48 ± 0.02
3	11.54 ± 1.36	3.91 ± 0.25	1.51 ± 0.42	9.63 ± 1.58	4.87 ± 0.05
4	>100	>100	5.01 ± 1.14	>100	33.07 ± 2.05
5	73.68 ± 2.08	6.37 ± 0.03	33.63 ± 1.39	56.91 ± 1.86	25.29 ± 1.34
CUR	9.89 ± 0.51	11.15 ± 1.05	2.71 ± 0.47	20.04 ± 2.61	11.55 ± 4.93
BZ	1.16 ± 0.04	1.28 ± 0.64	2.02 ± 0.12	4.12 ± 1.02	1.19 ± 0.25

Abbreviations: BZ, benznidazole (positive control for Chagas disease); CUR, curcumin (reference curcuminoid).

Table 2

In vitro anti-*T. cruzi* (amastigotes, CA-I/72 strain) activity of DBAs (IC_{50}), cytotoxicity in infected C2C12 cell line (CC_{50}) and selectivity index (SI) in the time-course evaluation

DBA	IC_{50}, CC_{50} (µM) ± SD and SI											
	8 h			12 h			24 h			48 h		
	IC_{50}	CC_{50}	SI	IC_{50}	CC_{50}	SI	IC_{50}	CC_{50}	SI	IC_{50}	CC_{50}	SI
1	>100	12.20 ± 1.15	ND	76.78 ± 1.39	2.00 ± 0.42	0.02	37.53 ± 1.01	0.28 ± 0.04	0.007	14.61 ± 1.10	0.03 ± 0.02	0.002
2	>100	40.73 ± 1.07	ND	>100	3.03 ± 0.79	ND	>100	0.33 ± 0.41	ND	>100	0.02 ± 0.03	ND
3	>100	29.81 ± 1.32	ND	63.30 ± 3.87	2.79 ± 0.30	0.04	62.08 ± 1.52	0.21 ± 0.13	0.003	3.72 ± 0.56	0.22 ± 0.17	0.05
4	>100	>100	ND	>100	60.41 ± 1.11	ND	>100	2.98 ± 0.24	ND	34.47 ± 0.94	0.66 ± 0.29	0.01
5	>100	93.29 ± 0.42	ND	>100	10.55 ± 1.26	ND	>100	0.30 ± 0.02	ND	>100	0.20 ± 0.01	ND
CUR	>100	60.34 ± 1.54	ND	>100	9.95 ± 1.17	ND	51.65 ± 1.26	1.88 ± 0.17	0.03	2.25 ± 0.65	0.47 ± 0.09	0.20
BZ	>10	>10	ND	6.85 ± 1.56	3.98 ± 0.31	0.58	5.97 ± 1.20	3.48 ± 0.70	0.58	1.54 ± 0.36	0.27 ± 0.07	0.17

Abbreviations: SI, selectivity index (values determined by CC_{50}/IC_{50}); BZ, benznidazole (positive control for Chagas disease); CUR, curcumin (reference curcuminoid); ND, not determined.
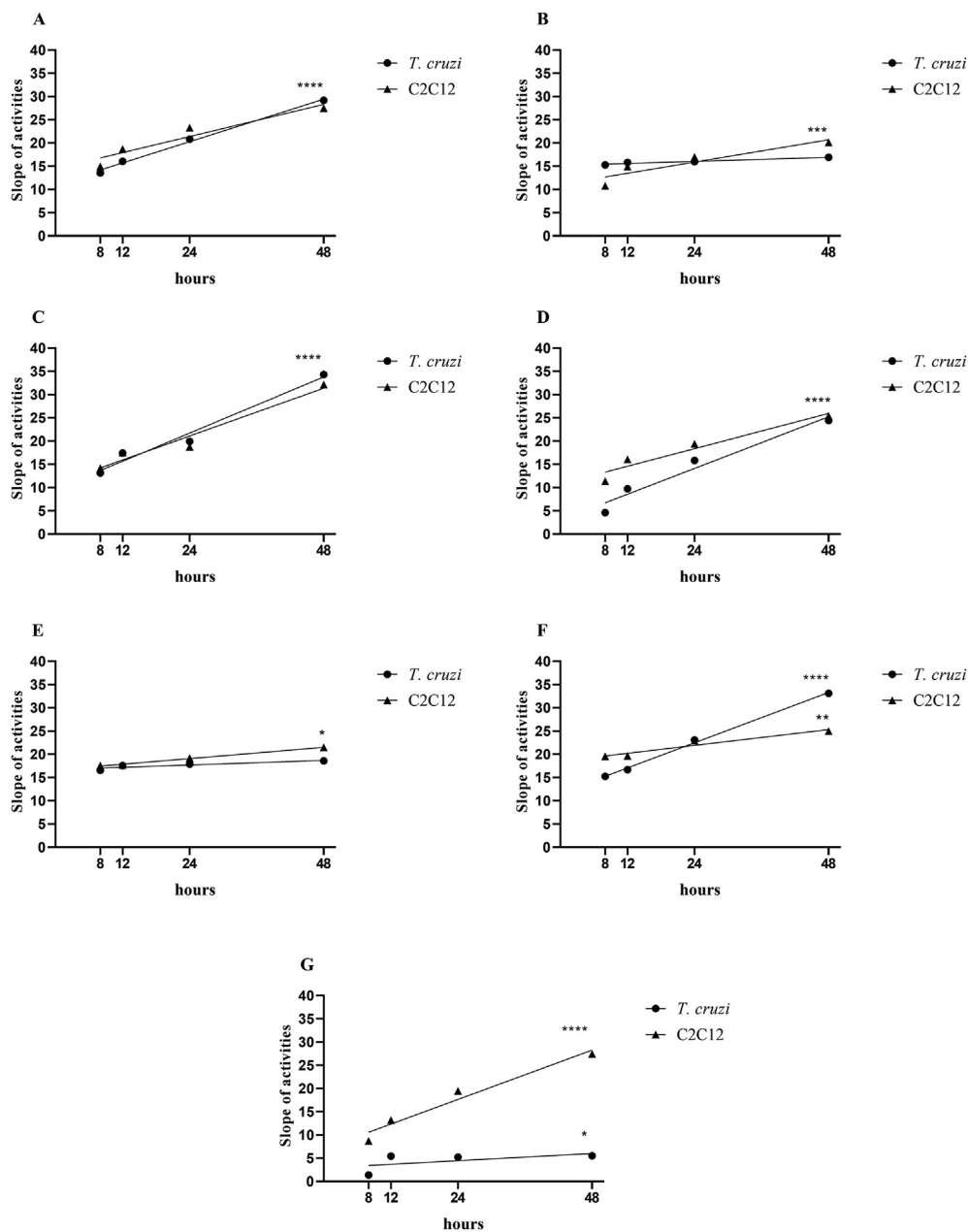

Fig. 2 Time-course statistical analysis of the anti-*T. cruzi* activity against intracelullar amastigotes form (CA-I/72 strain) and cytotoxic activity in C2C12-infected cells of dibenzalacetones (DBAs **1–5**) 1–5, curcumin (CUR) and benznidazole (BZ). **A** DBA **1**. **B** DBA **2**. **C** DBA **3**. **D** DBA **4**. **E** DBA **5**. **F** CUR. **G** BZ. *$P < 0.05$; **$P < 0.01$; ***$P < 0.001$; ****$P < 0.0001$.

Table 3

In vitro cytotoxicity activity (CC$_{50}$) of DBAs in infected C2C12 cell line and selectivity index (SI) after 72 h

Compound	CC$_{50}$ (μM) ± SD of infected C2C12 cells							
	Brazil strain		CA-I/72 strain		Sylvio X10/4 strain		Sylvio X10/7 strain	
	CC$_{50}$	SI	CC$_{50}$	SI	CC$_{50}$	SI	CC$_{50}$	SI
1	7.32 ± 0.41	0.35	5.74 ± 1.95	1.22	3.80 ± 0.24	0.11	3.29 ± 1.00	0.28
2	5.15 ± 0.13	0.10	4.30 ± 1.22	0.24	2.54 ± 1.86	0.05	0.90 ± 1.20	1.87
3	1.73 ± 0.05	0.43	1.62 ± 0.22	1.07	1.25 ± 0.02	0.13	1.15 ± 0.29	0.23
4	0.09 ± 0.11	ND	0.60 ± 0.16	0.12	0.11 ± 0.10	ND	0.37 ± 0.14	0.01
5	12.38 ± 2.29	2.25	15.46 ± 1.25	0.45	11.79 ± 7.74	0.20	4.06 ± 2.31	0.16
CUR	2.36 ± 1.24	0.20	6.71 ± 0.70	2.47	1.91 ± 0.02	0.09	3.37 ± 1.33	0.29
BZ	>10	ND	>10	ND	>10	ND	>10	ND

Abbreviations: SI, selectivity index (values determined by CC$_{50}$/IC$_{50}$ from intracellular amastigotes assays of the different strains after 72 h incubation); BZ, benznidazole (positive control for Chagas disease); CUR, curcumin (reference curcuminoid); ND, not determined.

Table 4

In vitro cytotoxicity activity (CC$_{50}$) of DBAs in non-infected C2C12 and LLC-MK2 cell lines and selectivity index (SI) after 72 h

DBA	CC$_{50}$ ± SD (μM)		SI	
	C2C12	LLC-MK$_2$	C2C12	LLC-MK$_2$
1	40.13 ± 1.25	16.57 ± 0.61	8.59	3.54
2	35.50 ± 0.50	31.39 ± 1.20	2.03	1.79
3	20.82 ± 0.67	11.51 ± 0.34	13.78	7.62
4	53.67 ± 1.26	50.10 ± 7.92	10.71	10.00
5	38.27 ± 1.69	38.12 ± 1.81	1.13	1.13
CUR	18.03 ± 0.42	32.49 ± 0.49	6.65	11.98
BZ	37.85 ± 1.54	167.50 ± 2.98	18.73	82.92

Abbreviations: SI, selectivity index (values determined by CC$_{50}$/IC$_{50}$ from intracellular amastigotes assay (72 h incubation, CA-I/72 strain)); BZ, benznidazole (positive control for Chagas disease); CUR, curcumin (reference curcuminoid).

Table 5

Effects of DBA **3** and CUR in female BALB/c mice for 14 days in the acute toxicity study

Groups	DA/TA	Mortality (%)	Latency to mortality (min)	Signs of toxicity
CN	0/5	0	–	None
DBA (**3**)$_{300}$	0/5	0	–	None
DBA (**3**)$_{1000}$	0/5	0	–	None
CUR$_{300}$	0/5	0	–	None
CUR$_{1000}$	0/5	0	–	None

Note: Signs of toxicity assessed: general appearance; ataxia; vocal fremitus; irritability; body tone; tremor; salivation; tearing; palpable ptosis; seizures; and abnormal movements.
Abbreviations: CN, control (vehicle, $n = 5$); DBA (**3**)$_{300}$, dose 300 mg/kg ($n = 5$); DBA (**3**)$_{1000}$, dose 1,000 mg/kg ($n = 5$); CUR$_{300}$, dose 300 mg/kg ($n = 5$); CUR$_{1000}$, dose 1,000 mg/kg ($n = 5$); DA, dead animals; TA, total animals.

showed highest SI values of 18.73 and 82.92 with C2C12 and LLC-MK$_2$ non-infected cell lines, respectively among all the compounds tested.

3.5. In vivo acute toxicity study in mice

DBA **3** and the reference CUR were further evaluated in an acute toxicity test in female BALB/C mice. Both compounds at oral doses 300 and 1,000 mg/kg produced no toxic effects as evidenced by the absence of general signs of toxicity (ataxia, vocal fremitus, irritability, body tone, tremor, salivation, palpable ptosis, seizures and abnormal movements) or mortality evaluated in the animals during the 14-day experimental period (Table 5).

4. Discussion

Curcumin is a widely studied phytochemical agent with anticancer, antiviral, antibacterial and antiparasitic activities, including against *Trypanosoma* parasites (Maghadamtousi et al., 2014; Salem et al., 2014; Cheraghipour et al., 2018). However, it is not a suitable candidate for the development of clinically useful drug because of its instability, poor absorption, and rapid elimination in the body. Currently, efforts are being made to identify clinically effective CUR analogs with improved pharmacokinetic profiles by modification of its chemical structure (Changtam et al., 2010; Chauhan et al., 2018; Carapina da Silva et al., 2019).

In the present study, we evaluated five DBAs (**1–5**) and identified DBA **3** as the most active compound against four strains of *T. cruzi* under the *in vitro* experimental conditions employed. In general, the CA-I/72 strain of *T. cruzi* was more susceptible than its Brazil, Sylvio X10/4 and Sylvio X10/7 strains when their intracellular amastigote forms were tested.

Due to the partial resistance of CA-I/72 strain against BZ (Nozaki et al., 1996) and the susceptibility to DBAs, the selected for the time-course study DBAs **1**, **3** and **4**, the reference compound CUR, and the positive control BZ, showed a time-dependent response against the intracellular amastigotes of the CA-I/72 strain of *T. cruzi*. However,

DBAs **2** and **5** did not show such time dependency in their activity as both were inactive.

It should be noted that there is a significant difference in the infection status (time of infection) of parasites used for the evaluation of the time-course of anti-*T. cruzi* activity and those used for trypanocidal activity against amastigote forms involving 72 h incubation periods. In the trypanocidal activity assay against amastigote and trypomastigote forms of parasites, mammalian cells and test samples were all added together at the beginning of incubation. In contrast, for the time-course evaluation, trypomastigotes were first incubated with mammalian cells for 48 h to transform them into amastigote forms and then test samples were added. This difference in the methodology used may account for the observed difference in the activity of the DBAs tested. This may enhance the indirect activity of the compounds against the parasites (see below).

The above effect can be related to the mechanism of elimination of parasites by host cells. Earlier studies have shown that the death of parasites *in vitro* by macrophages or cardiomyocytes can be triggered by the production of chemokines which is associated with the production of nitric oxide synthase (iNOS) and nitric oxide (NO) (Machado et al., 2000). While these effects are generally related to the protection of host cells, their overproduction can aggravate adverse pathology and lead to cell death (Titus et al., 1991). Previous studies have demonstrated both pro- and anti-oxidant activity of CUR, depending on the concentration used (Marathe et al., 2011). Thus, the above two factors can lead to higher toxicity against parasites and infected cells. Accordingly, all of the factors mentioned above can be responsible for the higher cytotoxic activity observed in the present study.

As discussed by Carapina da Silva et al. (2019), the use of SI has been suggested as an efficient way to analyze antiparasitic biological efficacy by comparing it with cytotoxicity. Thus, SI values ≥ 10 would be considered good, because these would indicate that the *in vitro* antiparasitic activity is not the result of an *in vitro* cytotoxicity. Other studies have also suggested SI ≥ 10 as a criterion for selection of hit compounds

against kinetoplastid protozoans (Ioset et al., 2009; Katsuno et al., 2015; Peña et al., 2015; Tempone et al., 2017; Linciano et al., 2018; Rolón et al., 2019; Martinez-Peinado et al., 2020). Additionally, the 2008 Drugs for Neglected Diseases Initiative workshop on experimental models in drug screening for Chagas disease has recommended determination of SI values during *in vitro* studies with trypomastigotes and intracellular amastigotes of *T. cruzi* parasites and comparing with those of the reference drug BZ (Romanha et al., 2010).

In these cytotoxicity studies, CUR which is considered safe to use in humans (Chainani-Wu, 2003; Chauhan et al., 2018) and DBA **1**, an approved sunscreen agent (Thaman et al., 1996), as well as the positive control drug BZ, showed CC_{50} values of 6.71–2.36, 7.32–3.29 and > 10, respectively, in infected C2C12 mammalian cells. Although DBAs **1–5** have shown cytotoxicity in infected C2C12 mammalian cells, due to the inherent high toxicity of the parasite in host cells, it is important to evaluate the toxicity of DBAs **1–5** in mammalian cells without parasitic infection. All DBAs tested showed lower cytotoxicity in non-infected C2C12 and LLC-MK2 cell lines (CC_{50} values of 53.67–11.51 μM). In general, DBAs **3** and **4** exhibited SI values > 10 when incubated with non-infected C2C12 cells. Similarly, SI values were ≥10 for DBA **4** and CUR when evaluated in non-infected LLC-MK2 cells. BZ exhibited no cytotoxicity in the non-infected cell lines tested.

The acute oral toxicity test aims to check for adverse effects in a short period after oral administration of a single dose of a substance or after multiple doses delivered over a period of 14 days (OECD, 2002). In the present *in vivo* study in mice, DBA **3** was well tolerated at single oral doses of 300 mg/kg and 1,000 mg/kg without any clinical toxicity signs throughout the 14-day experimental period. Moreover, during and after 14 days of acute single dosing, no animal died. Similar results were obtained with the reference curcumin-treated mice (single oral doses of 300 mg/kg and 1,000 mg/kg). An earlier cytotoxic study (Ohori et al., 2006) found a general good safety profile for a series of DBA compounds (which included DBA **3**) when tested in human hepatocytes. While studies with CUR in humans and experimental animals have shown it to be non-toxic (Chainani-Wu, 2003; Ohori et al., 2006; Chauhan et al., 2018), such toxicity data on DBA **3** are currently not available. However, it is noteworthy that in the MTT based cytotoxicity test on HeLa cell line, DBA **3** exhibited selective action against the malaria parasite *Plasmodium falciparum* with a therapeutic index of 166 (Aher et al., 2011). Also, DBA **3** was the most active among a series of DBA derivatives with growth suppression activity against human colon cancer cells (Ohori et al., 2006).

Our results with DBAs **1–4** based on IC_{50} and SI values, demonstrate that enhanced anti-*T. cruzi* activity is achievable by replacing the highly reactive β-diketone functionality in the CUR structure with monoketone moiety and by a selective addition of methoxy groups in the terminal aromatic rings. These structural modifications appear to facilitate formation of the extended phenoxyl radical ROS with the involvement of methoxy group oxygen (following *in situ* ionization and plausible O-demethylation in biological systems) in *para* positions of the terminal aromatic rings and the central methylene carbon chain (Litwinienko & Ingold, 2004). The ionization potential is highest when one of the methoxy groups is in *para* position of phenyl rings, as in DBA **3** which exhibited the highest anti-*T. cruzi* activity (Sakalyte et al., 2011). Interestingly, the potent antioxidant activity of DBAs **1**, **2** and **3** has been reported earlier (Handayani & Arty, 2008) and the parent compound DBA **1**, which blocks harmful UV rays, is a common ingredient currently used in sunscreens to adjust SPF values (Thaman et al., 1996).

Thus, DBA **3** showed the highest activity among all compounds tested against all *T. cruzi* strains. This DBA curcuminoid with methoxy groups in *para* (R3) and adjacent *meta* (R4) positions in the aromatic rings showed higher activity than both DBA **2** with methoxy group at *para* (R3) only and DBA **4** with methoxy groups at *para* (R3) and *ortho* (R1 and R4) positions in the terminal aromatic rings (which was inactive (IC_{50} > 100 μM) or showed low activity (IC_{50} = 33.06) against all strains of *T. cruzi* except for CA-I/72 strain with IC_{50} = 5.01 μM) as well as the

unsubstituted parent compound DBA **1**. Interestingly, DBA **3** has two oxygenated (methoxy) groups in its aromatic rings similar to those (methoxy and hydroxy) in the CUR molecule, namely the adjacent *para* (R3) and *meta* (R4) positions. The electron releasing methoxy and/or hydroxy groups in adjacent positions in aromatic rings are known to enhance the stability of ROS essential for the antiparasitic activity of CUR and its analogs (Pal & Bandyopadhyay, 2012). This may be attributable to the favorable steric interaction of these groups (Aher et al., 2011). In contrast, incorporation of electron withdrawing chlorine substituent in *para* position (R3) of aromatic rings, as in DBA **5**, generally lowered or completely abolished anti-*T. cruzi* activity.

The lipophilicity of DBAs also appears to play an important role in their anti-*T. cruzi* activity. Thus, DBA **3**, which is more lipophilic than CUR with two phenolic hydroxyl groups, exhibited higher anti-*T. cruzi* activity in these studies. Similar correlation between structure and lipophilicity with antioxidant activity essential for biological activities has been observed with other curcumin analogs (Shang et al., 2010).

By comparing the above anti-*T. cruzi* activity observed with CUR, DBA **1** and its non-phenolic, methoxy derivatives (DBAs **2–4**) and chloro derivative (DBA **5**), the following structure-activity relationships (SAR) can be deduced: (i) symmetry between the terminal aromatic rings is essential to form ROS; (ii) retention of bis(phenyl)heptadiene/pentadiene skeleton is crucial to elicit antiparasitic activity; (iii) *para, meta* and *ortho* positions in aromatic rings are useful to introduce additional functional groups to modify activity; (iv) addition of strong electron donating methoxy groups in aromatic rings increases antiparasitic activity, especially when *para* and *meta* positions are utilized together; and (v) introduction of electron withdrawing chlorine substituent in *para* position of aromatic rings leads to loss of activity.

The above SAR analysis indicates that the highest enhancement of the *in vitro* anti-*T. cruzi* activity in the present study is achieved by DBA **3** with a pentadiene monoketone symmetrical structure containing methoxy substituents at adjacent *para* and *meta* positions of the terminal aromatic rings. It is noteworthy that such enhanced *in vitro* and *in vivo* pharmacokinetic and cytotoxic profiles of tetramethoxy DBA compared to CUR have been recently reported (Liang et al., 2009). Similar SAR results with other curcuminoid analogs have also been observed with their anti-inflammatory (Arshad et al., 2017), anticancer (Shetty et al., 2015), antimicrobial (Vieira et al., 2018) and antiparasitic (Alkhaldi et al., 2015) activities. Interestingly, these diverse biological activities of CUR analogs are related to their antioxidant potency.

Some of the DBA curcuminoids investigated in this study were previously evaluated against other protozoan parasites and oral disease-causing bacteria. DBAs **1**, **2** and **5** exhibited moderate antimicrobial activity (MIC = 100 μg/ml) against several *Streptococcus* species (Vieira et al., 2018). In another study, among the DBAs **1**, **2** and **5** that showed antiparasitic activity against *Trichomonas vaginalis*, DBA **1** was the most active with a 98.8% reduction in the parasitic viability after 24 h incubation with an IC_{50} value of 50 μM (Carapina da Silva et al., 2019). Additionally, DBA **3** was the most active among a series of twelve DBA compounds tested against *P. falciparum* (both chloroquine-sensitive and chloroquine-resistant strains, IC_{50} of 1.97 and 1.69 μM, respectively) (Aher et al., 2011).

Compounds with IC_{50} values < 10 μM in *in vitro* experiments with infective protozoan parasites are considered as a hit and lead candidates for further *in vivo* evaluations (Katsuno et al., 2015). In the present study, DBA **3** consistently showed IC_{50} values < 10 μM under *in vitro* conditions in all four strains of *T. cruzi* which qualifies it as a hit and lead compound for further *in vivo* studies. Additional support for this selection comes from the time-course analysis of its *in vitro* antitrypanosomal activity. Diveratralacetone, with a 5-carbon monoketone linker between terminal non-phenolic rings, is more stable and should have better bioavailability profile than CUR, with a 7-carbon diketone linker between its terminal phenolic rings. A study in mice (Pan et al., 1999) found glucuronidation of phenolic OH in CUR to be the major metabolic pathway (99% of i.p. dose) and its oral dose resulted in very low absorption (90% less than i.p.

dose) into blood. However, such biotransformation may not be relevant for the bioavailability of DBA **3** since it is a non-phenolic compound (Tamvakopoulos et al., 2007).

Finally, pharmacokinetic studies in animals and humans are needed as the DBAs (the present study and Chauhan et al., 2020) progress to *in vivo* phase to establish route and dosage for potential treatment of trypanosomiasis and leishmaniasis. Based on the *in vitro* results, the following comments may be made regarding this: (i) DBA **1** compared favorably under *in vitro* conditions to antileishmanial drug miltefosine which is orally effective (Chauhan et al., 2018); (ii) based on the current use of DBA **1** as a sunscreen agent, its topical application in treating parasitic diseases has been suggested (Chauhan et al., 2020); and (iii) in addition to oral dosing similar to BZ (for CD) and miltefosine (for visceral leishmaniasis), diveratralacetone should also be amenable to topical administration; such topical ointments containing turmeric and CUR are commonly used in herbal medical practice (Cheraghipour et al., 2018).

5. Conclusions

To the best of our knowledge, the present study establishes for the first time the versatile anti-*T. cruzi* activity of monoketone, non-phenolic DBA analogs of CUR against multiple strains of the parasite. Among the DBAs evaluated, we have identified DBA **3** (diveratralacetone) as a hit compound for further *in vivo* studies against *T. cruzi* parasites. Although DBA **3** showed higher cytotoxicity in infected mammalian cells tested under *in vitro* conditions when compared to BZ, its toxicity profile is comparable to CUR, the reference compound. Moreover, our preliminary *in vivo* acute toxicity study in a mouse model, reported herein, indicated the safety of diveratralacetone which is comparable to CUR. Thus, based on the *in vitro* antitrypanosomal activity of DBA and its analogs, we conclude that diveratralacetone is a suitable candidate to further optimize and evaluate *in vivo* its potential to treat Chagas disease.

Ethical approval

All experiments were authorized by the University of Franca's Ethics Committee for Animal Care (Approval number: 049/15). All animals were handled using good animal practice as defined by the University of Franca in concordance with Brazilian legislation.

CRediT author statement

Julia M. Souza: Methodology, Formal Analysis, Investigation, Writing – original draft. Tatiana M. Vieira: Formal Analysis, Investigation, Ana C. B. B. Candido: Investigation. Daiane Y. Tezuka: Investigation. G. Subba Rao: Methodology, Writing – review & editing. Sérgio de Albuquerque: Resources. Antônio E. M. Crotti: Methodology, Writing – review & editing. Jair L. Siqueira-Neto: Methodology, Resources, Writing – review & editing, Supervision, Funding acquisition. Lizandra G. Magalhães: Resources, Writing – review & editing, Supervision, Funding acquisition.

Declaration of competing interests

The authors declare that they have no known competing financial interests or personal relationships that could have appeared to influence the work reported in this paper.

References

Aggarwal, M.L., Chacko, K.M., Kuruvilla, B.T., 2016. Systematic and comprehensive investigation of the toxicity of curcuminoid-essential oil complex: A bioavailable turmeric formulation. Mol. Med. Rep. 13, 592–604. https://doi.org/10.3892/mmr.2015.4579.

Aher, R.B., Wanare, G., Kawathekar, N., Kumar, R.R., Kaushik, N.K., Sahal, D., Chauhan, V.S., 2011. Dibenzylideneacetone analogues as novel *Plasmodium falciparum* inhibitors. Bioorganic Med. Chem. Lett. 21, 3034–3036. https://doi.org/10.1016/j.bmcl.2011.03.037.

Alkhaldi, A.A.M., Creek, D.J., Ibrahim, H., Kim, D.-H., Quashie, N.B., Burgess, K.E., et al., 2015. Potent trypanocidal curcumin analogs bearing a monoenone linker motif act on *Trypanosoma brucei* by forming an adduct with trypanothione. Mol. Pharmacol. 87, 451–464. https://doi.org/10.1124/mol.114.096016.

Arshad, L., Areeful Haque, M., Bukhari, S.N.A., Jantan, I., 2017. An overview of structure-activity relationship studies of curcumin analogs as antioxidant and anti-inflammatory agents. Future Med. Chem. 9, 605–626. https://doi.org/10.4155/fmc-2016-0223.

Bern, C., 2015. Chagas' disease. N. Engl. J. Med. 373, 456–466. https://doi.org/10.1056/NEJMra1410150.

Carapina da Silva, C., Pacheco, B.S., das Neves, R.N., Dié Alves, M.S., Sena-Lopes, Â., Moura, S., et al., 2019. Antiparasitic activity of synthetic curcumin monocarbonyl analogues against *Trichomonas vaginalis*. Biomed. Pharmacother. 111, 367–377. https://doi.org/10.1016/j.biopha.2018.12.058.

Cas, M.D., Ghidoni, R., 2019. Dietary curcumin: Correlation between bioavailability and health potential. Nutrients 11, 2147. https://doi.org/10.3390/nu11092147.

Chainani-Wu, N., 2003. Safety and anti-inflammatory activity of curcumin: A component of tumeric (*Curcuma longa*). J. Altern. Complement. Med. 9, 161–168. https://doi.org/10.1089/107555303321223035.

Chakraborti, S., Dhar, G., Dwivedi, V., Das, A., Poddar, A., Chakraborti, G., et al., 2013. Stable and potent analogues derived from the modification of the dicarbonyl moiety of curcumin. Biochemistry 52, 7449–7460. https://doi.org/10.1021/bi400734e.

Changtam, C., de Koning, H.P., Ibrahim, H., Sajid, M.S., Gould, M.K., Suksamrarn, A., 2010. Curcuminoid analogs with potent activity against *Trypanosoma* and *Leishmania* species. Eur. J. Med. Chem. 45, 941–956. https://doi.org/10.1016/j.ejmech.2009.11.035.

Chauhan, I.S., Marwa, S., Rao, G.S., Singh, N., 2020. Antiparasitic dibenzalacetone inhibits the GTPase activity of Rab 6 protein of *Leishmania donovani* (LdRab6), a potential target for its antileishmanial effect. Parasitol. Res. 119, 2991–3003. https://doi.org/10.1007/s00436-020-06810-4.

Chauhan, I.S., Rao, G.S., Shankar, J., Chauhan, L.K.S., Kapadia, G.J., Singh, N., 2018. Chemoprevention of leishmaniasis: *In vitro* antiparasitic activity of dibenzalacetone, a synthetic curcumin analog leads to apoptotic cell death in *Leishmania donovani*. Parasitol. Int. 67, 627–636. https://doi.org/10.1016/j.parint.2018.06.004.

Cheraghipour, K., Marzban, A., Ezatpour, B., Khanizadeh, S., Koshki, J., 2018. Antiparasitic properties of curcumin: A review. AIMS Agric. Food 3, 561–578. https://doi.org/10.3934/agrfood.2018.4.561.

de Menezes, D. da R., Calvet, C.M., Rodrigues, G.C., de Souza Pereira, M.C., Almeida, I.R., de Aguiar, et al., 2016. Hydroxamic acid derivatives: A promising scaffold for rational compound optimization in Chagas disease. J. Enzyme Inhib. Med. Chem. 31, 964–973. https://doi.org/10.3109/14756366.2015.1077330.

Ekins, S., Lage de Siqueira-Neto, J., McCall, L.-I., Sarker, M., Yadav, M., Ponder, E.L., et al., 2015. Machine learning models and pathway genome data base for *Trypanosoma cruzi* drug discovery. PLoS Negl. Trop. Dis. 9, e0003878 https://doi.org/10.1371/journal.pntd.0003878.

Elamin, M., Al-Olayan, E., Abdel-Gaber, R., Yehia, R.S., 2021. Anti-proliferative and apoptosis induction activities of curcumin on *Leishmania major*. Rev. Argent. Microbiol. 1–8. https://doi.org/10.1016/j.ram.2020.08.004.

Gressler, L.T., Oliveira, C.B., Coradini, K., Rosa, L.D., Grando, T.H., Baldissera, M.D., et al., 2015. Trypanocidal activity of free and nanoencapsulated curcumin on *Trypanosoma evansi*. Parasitology 142, 439–448. https://doi.org/10.1017/S0031182014001292.

Guarner, J., 2019. Chagas disease as example of a reemerging parasite. Semin. Diagn. Pathol. 36, 164–169. https://doi.org/10.1053/j.semdp.2019.04.008.

Handayani, S., Arty, I.S., 2008. Synthesis of hydroxyl radical scavengers from benzalacetone and its derivatives. J. Phys. Sci. 19, 61–68.

Ioset, J.-R., Brun, R., Wenzler, T., Kaiser, M., Yardley, V., 2009. Drug screening for kinetoplastid diseases: A training manual for screening in neglected diseases. DNDi Pan-Asian Screen. Netw. http://www.dndi.org/images/stories/pdf_scientific_pub/2009/kinetoplastid_drug_screening_manual_final.pdf.

Katsuno, K., Burrows, J.N., Duncan, K., Huijsduijnen, R.H. Van, Kaneko, T., et al., 2015. Hit and lead criteria in drug discovery for infectious diseases of the developing world. Nat. Rev. Drug Discov. 14, 751–758. https://doi.org/10.1038/nrd4683.

Leow, P.C., Bahety, P., Boon, C.P., Lee, C.Y., Tan, K.L., Yang, T., Ee, P.L.R., 2014. Functionalized curcumin analogs as potent modulators of the Wnt/β-catenin

signaling pathway. Eur. J. Med. Chem. 71, 67–80. https://doi.org/10.1016/j.ejmech.2013.10.073.

Liang, G., Shao, L., Wang, Y., Zhao, C., Chu, Y., Xiao, J., et al., 2009. Exploration and synthesis of curcumin analogues with improved structural stability both *in vitro* and *in vivo* as cytotoxic agents. Bioorganic Med. Chem. 17, 2623–2631. https://doi.org/10.1016/j.bmc.2008.10.044.

Linciano, P., Moraes, C.B., Alcantara, L.M., Franco, C.H., Pascoalino, B., Freitas-Junior, L.H., et al., 2018. Aryl thiosemicarbazones for the treatment of trypanosomatidic infections. Eur. J. Med. Chem. 146, 423–434. https://doi.org/10.1016/j.ejmech.2018.01.043.

Litwinienko, G., Ingold, K.U., 2004. Abnormal solvent effects on hydrogen atom abstraction. 2. Resolution of the curcumin antioxidant controversy. The role of sequential proton loss electron transfer. J. Org. Chem. 69, 5888–5896. https://doi.org/10.1021/jo049254j.

Londero, V.S., da Costa-Silva, T.A., Gomes, K.S., Ferreira, D.D., Mesquita, J.T., Tempone, A.G., et al., 2018. Acetylenic fatty acids from *Porcelia macrocarpa* (Annonaceae) against trypomastigotes of *Trypanosoma cruzi*: Effect of octadec-9-ynoic acid in plasma membrane electric potential. Bioorg. Chem. 78, 307–311. https://doi.org/10.1016/j.bioorg.2018.03.025.

Machado, F.S., Martins, G.A., Aliberti, J.C.S., Mestriner, F.L.A.C., Cunha, F.Q., Silva, J.S., 2000. *Trypanosoma cruzi*-infected cardiomyocytes produce chemokines and cytokines that trigger potent nitric oxide-dependent trypanocidal activity. Circulation 102, 3003–3008. https://doi.org/10.1161/01.CIR.102.24.3003.

Magalhães, L.G., Machado, C.B., Morais, E.R., Bueno De Carvalho Moreira, É., Soares, C.S., Da Silva, S.H., et al., 2009. *In vitro* schistosomicidal activity of curcumin against *Schistosoma mansoni* adult worms. Parasitol. Res. 104, 1197–1201. https://doi.org/10.1007/s00436-008-1311-y.

Maghadamtousi, S.Z., Kadir, H.A., Hassandarvish, P., Tajik, H., Abubakar, S., Zandi, K., 2014. 2014. A review on antibacterial, antiviral, and antifungal activity of curcumin. Biomed Res. Int. 186864. https://doi.org/10.1155/2014/186864.

Marathe, S.A., Dasgupta, I., Gnanadhas, D.P., Chakravortty, D., 2011. Multifaceted roles of curcumin: Two sides of a coin! Expert Opin. Biol. Ther. 11, 1485–1499. https://doi.org/10.1517/14712598.2011.623124.

Martinez-Peinado, N., Cortes-Serra, N., Torras-Claveria, L., Pinazo, M.J., Gascon, J., Bastida, J., Alonso-Padilla, J., 2020. Amaryllidaceae alkaloids with anti-*Trypanosoma cruzi* activity. Parasit. Vectors 13, 299. https://doi.org/10.1186/s13071-020-04171-6.

Nelson, K.M., Dahlin, J.L., Bisson, J., Graham, J., Pauli, G.F., Walters, M.A., 2017. The essential medicinal chemistry of curcumin. J. Med. Chem. 60, 1620–1637. https://doi.org/10.1021/acs.jmedchem.6b00975.

Nozaki, T., Engel, J., Dvorak, J., 1996. Cellular and molecular biological analyses of nifurtimox resistance in *Trypanosoma cruzi*. Am. J. Trop. Med. Hyg. 5, 111–117. https://doi.org/10.4269/ajtmh.1996.55.111.

OECD, 2002. Test No. 420: acute oral toxicity - fixed dose procedure. OECD Guidelines for the Testing of Chemicals, Section 4. OECD Publishing, Paris. https://doi.org/10.1787/9789264070943-en.

Ohori, H., Yamakoshi, H., Tomizawa, M., Shibuya, M., Kakudo, Y., Takahashi, A., et al., 2006. Synthesis and biological analysis of new curcumin analogues bearing an enhanced potential for the medicinal treatment of cancer. Mol. Cancer Ther. 5, 2563–2571. https://doi.org/10.1158/1535-7163.MCT-06-0174.

Pal, C., Bandyopadhyay, U., 2012. Redox-active antiparasitic drugs. Antioxid. Redox Signal. 17, 555–582. https://doi.org/10.1089/ars.2011.4436.

Pan, M.H., Huang, T.M., Lin, J.K., 1999. Biotransformation of curcumin through reduction and glucuronidation in mice. Drug Metab. Dispos. 27, 486–494.

Peña, I., Pilar Manzano, M., Cantizani, J., Kessler, A., Alonso-Padilla, J., Bardera, A.I., et al., 2015. New compound sets identified from high throughput phenotypic screening against three kinetoplastid parasites: An open resource. Sci. Rep. 5, 1–12. https://doi.org/10.1038/srep08771.

Pereira, R.M., Greco, G.M.Z., Moreira, A.M., Chagas, P.F., Caldas, I.S., Gonçalves, R.V., Novaes, R.D., 2017. Applicability of plant-based products in the treatment of *Trypanosoma cruzi* and *Trypanosoma brucei* infections: A systematic review of preclinical *in vivo* evidence. Parasitology 144, 1275–1287. https://doi.org/10.1017/S0031182017000634.

Pérez-Molina, S.A., Molina, I., 2018. Chagas disease. Lancet 391, 82–94. https://doi.org/10.1016/S0140-6736(17)31612-4.

Postan, M., Dvorak, J.A., Mcdaniel, J.P., 1983. Studies of *Trypanosoma cruzi* clones in inbred mice. Am. J. Trop. Med. Hyg. 32, 497–506. https://doi.org/10.4269/ajtmh.1983.32.497.

Raether, W., Seidenath, H., 1983. The activity of fexinidazole (HOE 239) against experimental infections with *Trypanosoma cruzi*, trichomonads and *Entamoeba histolytica*. Ann. Trop. Med. Parasitol. 77, 13–26. https://doi.org/10.1080/00034983.1983.11811668.

Rassi Jr., A., Rassi, A., Marin-Neto, J.A., 2010. Chagas disease. Lancet 375, 1388–1402. https://doi.org/10.1016/S0140-6736(10)60061-X.

Reddy, R.C., Vatsala, P.G., Keshamouni, V.G., Padmanaban, G., Rangarajan, P.N., 2005. Curcumin for malaria therapy. Biochem. Biophys. Res. Commun. 326, 472–474. https://doi.org/10.1016/j.bbrc.2004.11.051.

Rolón, M., Lima, A.P. de A., Coronel, C., Vega, M.C., Pandolfi, E., de Arias, A.R., 2019. The efficacy of new 2,5-dihydroxybenzyl derivatives against *Trypanosoma cruzi, Leishmania infantum* and *Leishmania braziliensis*. J. Infect. Dev. Ctries. 13, 565–576. https://doi.org/10.3855/jidc.10622.

Romanha, A.J., de Castro, S.L., Soeiro, M. de N.C., Lannes-Vieira, J., Ribeiro, I., Talvani, A., et al., 2010. *In vitro* and *in vivo* experimental models for drug screening and development for Chagas disease. Mem. Inst. Oswaldo Cruz 105, 233–238. https://doi.org/10.1590/S0074-02762010000200022.

Sakalyte, A., Simokaitiene, J., Tomkeviciene, A., Keruckas, J., Buika, G., Grazulevicius, J.V., et al., 2011. Effect of methoxy substituents on the properties of the derivatives of carbazole and diphenylamine. J. Phys. Chem. C 115, 4856–4862. https://doi.org/10.1021/jp109643r.

Saldanha, G.B., Saldanha, G.B., de Sousa, M.R.S.C., Oliveira, G.L.D.S., da Silva, A.P.D.S.C.L., David, J.M., David, J.P., 2018. Absence of toxicity in Swiss mice following treatment with 7-acetoxy-4-aryl-3,4-dihydrocoumarin: Acute and repeated-dose toxicity study. Regul. Toxicol. Pharmacol. 94, 75–82. https://doi.org/10.1016/j.yrtph.2018.01.003.

Salem, M., Rohani, S., Gillies, E.R., 2014. Curcumin, a promising anti-cancer therapeutic: A review of its chemical properties, bioactivity and approaches to cancer cell delivery. RSC Adv. 4, 10815–10829. https://doi.org/10.1039/c3ra46396f.

Shang, Y.-J., Jin, X.-L., Shang, X.-L., Tang, J.-J., Liu, G.-Y., Dai, F., et al., 2010. Antioxidant capacity of curcumin-directed analogues: Structure-activity relationship and influence of microenvironment. Food Chem. 119, 1435–1442. https://doi.org/10.1016/j.foodchem.2009.09.024.

Shetty, D., Kim, Y.J., Shim, H., Snyder, J.P., 2015. Eliminating the heart from the curcumin molecule: Monocarbonyl curcumin mimics (MACs). Molecules 20, 249–292. https://doi.org/10.3390/molecules20010249.

da Silva, A.P., Oliveira, G.L., Medeiros, S.C., Sousa, A.M., Lopes, L.D.S., David, J.M., da Costa, J.S., De Freitas, R.M., 2016. Pre-clinical toxicology of garcinielliptone FC, a tautomeric pair of polyprenylated benzophenone, isolated from *Platonia insignis* Mart seeds. Phytomedicine 23, 477–482. https://doi.org/10.1016/j.phymed.2016.02.013.

Stevens, J.R., 2008. Kinetoplastid phylogenetics, with special reference to the evolution of parasitic trypanosomes. Parasite 15, 226–232. https://doi.org/10.1051/parasite/2008153226.

Tamvakopoulos, C., Dimas, K., Sofianos, Z.D., Hatziantoniou, S., Han, Z., Liu, Z.L., et al., 2007. Metabolism and anticancer activity of the curcumin analogue, dimethoxycurcumin. Clin. Cancer Res. 13, 1269–1277. https://doi.org/10.1158/1078-0432.CCR-06-1839.

Tempone, A.G., Ferreira, D.D., Lima, M.L., Costa Silva, T.A., Borborema, S.E.T., Reimão, J.Q., et al., 2017. Efficacy of a series of alpha-pyrone derivatives against *Leishmania* (*L.*) *infantum* and *Trypanosoma cruzi*. Eur. J. Med. Chem. 139, 947–960. https://doi.org/10.1016/j.ejmech.2017.08.055.

Thaman, L.A., Deckner, G.E., Sottery, J.P., 1996. Photoprotection compositions having improved efficiency. US Patent 5516508A.

Titus, R.G., Sherry, B., Cerami, A., 1991. The involvement of TNF, IL-1 and IL-6 in the immune response to protozoan parasites. Immunol. Today 12, 13–16. https://doi.org/10.1016/S0167-5699(05)80005-2.

Vanchinathan, K., Bhagavannarayana, G., Muthu, K., Meenakshisundaram, S.P., 2011. Synthesis, crystal growth and characterization of 1,5-diphenylpenta-1,4- dien-3-one: An organic crystal. Phys. B Condens. Matter 406, 4195–4199. https://doi.org/10.1016/j.physb.2011.07.055.

Vieira, T.M., dos Santos, I.A., Silva, T.S., Martins, C.H.G., Crotti, A.E.M., 2018. Antimicrobial activity of monoketone curcuminoids against cariogenic bacteria. Chem. Biodivers. 15, 5–12. https://doi.org/10.1002/cbdv.201800216.

Weber, W.M., Hunsaker, L.A., Abcouwer, S.F., Deck, L.M., Jagt, D.L.V., 2005. Anti-oxidant activities of curcumin and related enones. Bioorganic Med. Chem. 13, 3811–3820. https://doi.org/10.1016/j.bmc.2005.03.035.